Nanostructure Formation and Passivation of Large-Area Black Silicon for Solar Cell Applications

*Yaoping Liu, Tao Lai, Hailing Li, Yan Wang, Zengxia Mei, Huili Liang, Zhilei Li, Fengming Zhang, Wenjing Wang, Andrej Yu Kuznetsov, and Xiaolong Du**

***N**anoscale textured silicon and its passivation are explored by simple low-cost metal-assisted chemical etching and thermal oxidation, and large-area black silicon was fabricated both on single-crystalline Si and multicrystalline Si for solar cell applications. When the Si surface was etched by $HF/AgNO_3$ solution for 4 or 5 min, nanopores formed in the Si surface, 50–100 nm in diameter and 200–300 nm deep. The nanoscale textured silicon surface turns into an effective medium with a gradually varying refractive index, which leads to the low reflectivity and black appearance of the samples. Mean reflectance was reduced to as low as 2% for crystalline Si and 4% for multicrystalline Si from 300 to 1000 nm, with no antireflective (AR) coating. A black-etched multicrystalline-Si of 156 mm × 156 mm was used to fabricate a primary solar cell with no surface passivation or AR coating. Its conversion efficiency (η) was 11.5%. The cell conversion efficiency was increased greatly by using surface passivation process, which proved very useful in suppressing excess carrier recombination on the nanostructured surface. Finally, a black m-Si cell with efficiency of 15.8% was achieved by using SiO_2 and SiN_X bilayer passivation structure, indicating that passivation plays a key role in large-scale manufacture of black silicon solar cells.*

Dr. Y. Liu, Y. Wang, Dr. Z. Mei, H. Liang, Prof. X. Du
Beijing National Laboratory for Condensed Matter Physics Institute of Physics
Chinese Academy of Sciences
Beijing 100190, PR China
E-mail: xldu@aphy.iphy.ac.cn
T. Lai, Z. Li, Prof. F. Zhang
Tianwei New Energy Holdings Co., Ltd
Chengdu 610200, PR China
H. Li, Prof. W. Wang
Institute of Electrical Engineering
Chinese Academy of Sciences
Beijing 100190, PR China
Prof. A. Y. Kuznetsov
Department of Physics
University of Oslo
NO-0316 Oslo, Norway

DOI: 10.1002/smll.201101792

1. Introduction

In recent decades, nanostructured Si surfaces have been extensively explored for their prominent light-trapping features, which may increase the efficiency of Si solar cells by means of lowering their reflectivity and maximizing the absorption of incident photons. Commonly, silicon (Si) surfaces have a naturally high reflectivity with a strong spectral dependence,[1,2] and surface texturing has to be used to reduce the light loss, such as micron-size pyramidal dots formed by anisotropic etching on crystalline-Si (c-Si) solar cells. This technique cannot be applied to multicrystalline-Si (m-Si) wafers however, because they consist of crystallites with different orientations.[3,4] In such cases very common acidic etchants enable isotropic fast etching of m-Si surface. Usually, the mean reflectance (R) is greater than 10% for pyramid-textured c-Si surfaces and greater than 20% for

NANO MICRO small

textured m-Si, in the wavelength range 300 to 1000 nm.[4] The reflectance can be further reduced by a quarter-wavelength antireflective (AR) coating applied to the top surface of Si. However, even with AR coating, chemically textured surfaces still show reflection losses of about 5–10%, and they also demonstrate a strong angle dependence in a narrow spectral range.[5]

Efficient reflection suppression across a broad spectral range and less angle dependence can be achieved when the textured scale is either nanoscale or smaller than the wavelength of incident light.[6] The most important reason is that the nanoscale textured silicon surface has a gradually varying refractive index, resulting in low reflectivity and a black appearance.[1,7] Various methods have been developed to texture the silicon surface at the nanometer scale, which is usually referred to as making "black silicon."[2,8–13] Both ultrafast-laser textured surfaces and reactive-ion-etched Si surfaces have very low reflectance across a broad spectrum, but they are not suitable for commercial large-area "black silicon" solar cells because of their inefficient and complicated fabrication processes.

We adopted a simple chemical method to fabricate large-area black silicon for solar cell applications.[14] First, noble metal nanoparticles (Pt, Au, Ag, Cu) are deposited on Si substrate by thermal evaporation, then the Si wafer is immersed in an aqueous solution of HF and H_2O_2 for several minutes. After the metal particles are removed, a black non-reflecting Si wafer is obtained with very low reflectivity across a broad spectral range and with evident applicability in solar cells. This technique can be applied to various structural forms of single- or multi-crystalline bulk silicon, as well as to amorphous or microcrystalline thin Si films.[14,15] Because of the very thin and nearly uniform texture layer (only 200–300 nm on the top surface of the wafer), which is the reason for the very low reflectivity, this chemical texturing method is very suitable for next-generation ultrathin (less than 100 μm) wafers (c-Si and m-Si) and thin-film (less than 5 μm) silicon solar cells.[5] Unfortunately, an expensive vacuum evaporation system is indispensable for the deposition of metal nanoparticles, and this is the main obstacle for fabricating large-area black silicon at low cost.

Very recently, a graded-index "black silicon" surface was obtained by cheap one-step nanoparticle-catalyzed liquid etching without using the expensive vacuum evaporation system for nanoparticle deposition.[16] Polished p-type Si (100) substrate with resistivity of 1–2 Ω cm is immersed in 0.4 mM $HAuCl_4$ solution, an equal quantity of $HF/H_2O_2/H_2O$ 1:5:2 mixture is added, and the combination is then sonicated for several minutes. After that, surface gold contamination can be removed in I_2/KI or aqua regia. The $HAuCl_4$ black-etching was found to reduce (100) silicon surface reflectance to below 2% from 300 to 1000 nm, with no antireflective coating.[16] A crystalline black silicon solar cell with 16.8% efficiency was obtained by incorporating a density-graded nanoporous surface layer made by one-step nanoparticle-catalyzed etching. Its reflectance was less than 3% within the solar spectrum, with no AR coating.[17] However, $HAuCl_4$ is still too expensive to realize large-area black silicon fabrication for commercial products, and the excess surface recombination must be suppressed. In this letter, we report an even cheaper method that uses $AgNO_3$ to fabricate large-area black silicon on both non-polished commercial c-Si and m-Si, and several solar cells were also fabricated based on the black-etched 156 mm × 156 mm m-Si with surface passivation. The cost of $AgNO_3$ is only about 1% that of $HAuCl_4$, so $AgNO_3$ is more promising for commercial fabrication of black-silicon-based solar cells.

Both commercially used 125 mm × 125 mm c-Si and 156 mm × 156 mm m-Si are p-type with resistivity of 1–3 Ω cm and thickness of 200 ± 20 μm. Before the black-etching in a solution of $AgNO_3$ and HF, the c-Si and m-Si were immersed in 15% NaOH and then in $HNO_3/HF/CH_3COOH$, to remove the saw damage on the Si surface.[2] The black silicon was obtained by stain etching in a polytetrafluoroethene container which was filled with 4.0 M HF and 0.01 M $AgNO_3$ solution at room temperature. The etching time ranged from 30 s to 5 min. After etching, the surface silver contamination was removed by HNO_3 in a sonication bath, then the silicon wafers were rinsed with deionized water and dried by blowing nitrogen. Hemispheric total reflectance for normal incidence was measured on a Varian Cary 5000 spectrophotometer with an integrating sphere. The morphology and structures of the samples were characterized with Hitachi S-4800 scanning electron microscopy (SEM). The cell efficiency was measured by using Halm cetisPV-CT-L1. The EQE was measured by using PV Measurement System QEX7.

2. Results and Discussion

Figure 1 shows the hemispheric total reflectance spectra of the p-Si (100) wafer, before and after being etched for different durations from 30 s to 5 min.The mean reflectance of the non-etched p-Si (100) wafer is about 40% from 300 to 1000 nm. Subsequently, the average reflectance decreased to 24% when the c-Si is etched in the $HF/AgNO_3$ solution for 30 s. With increasing etching time the reflectance decreases gradually. The lowest reflectance is about 2% after the p-Si (100) wafer is etched in the $HF/AgNO_3$ solution for 5 min.

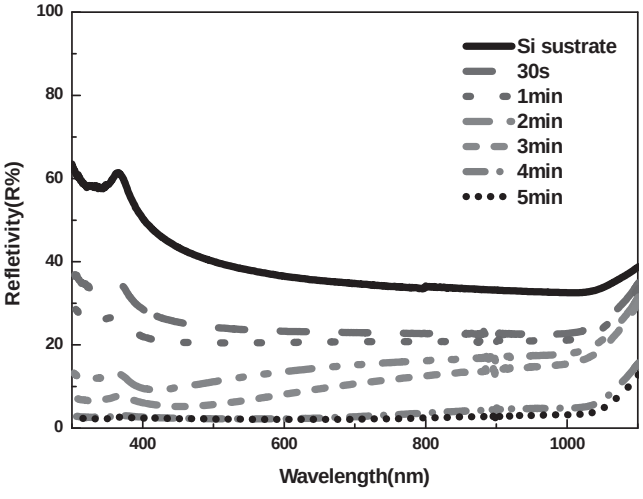

Figure 1. Hemispheric total reflectance of the p-Si (100) wafer, before and after being etched in $HF/AgNO_3$ solution from 30 s to 5 min.

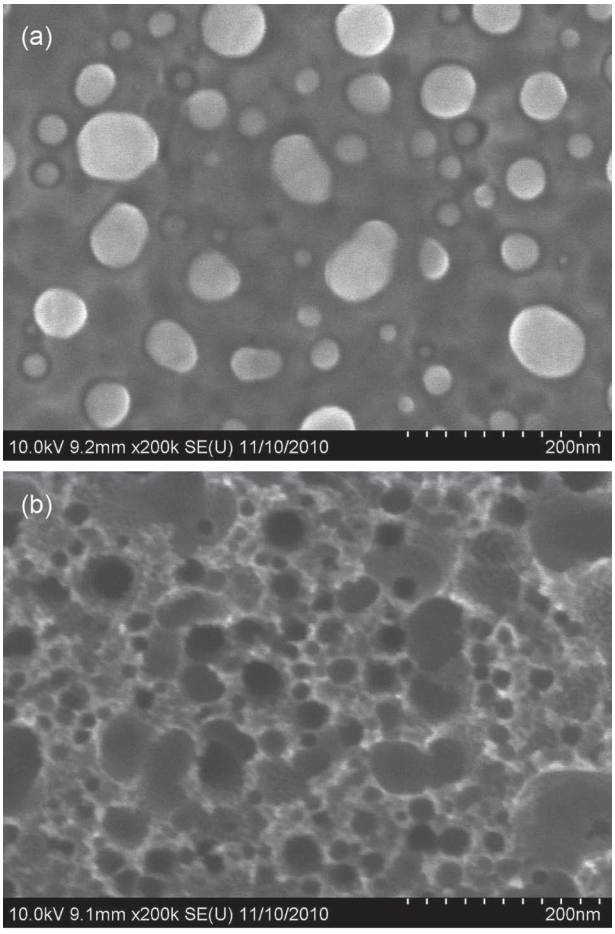

Figure 2. a) SEM image of Ag particles on silicon etched by $HF/AgNO_3$ solution for 30 s. b) Shallow nanopores formed in the top surface of Si substrate after the Ag is removed.

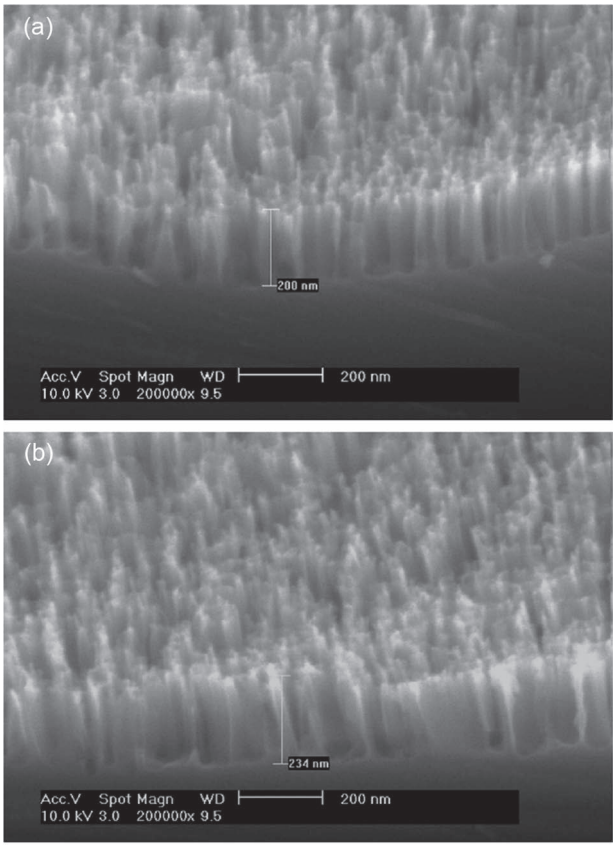

Figure 3. Cross-sectional SEM images of the p-Si (100) surface etched in $HF/AgNO_3$ solution for: a) 4, and, b) 5 min after Ag is removed.

Figure 2a shows an SEM image of the p-Si (100) surface after being etched in $HF/AgNO_3$ solution for 30 s before removing the silver by HNO_3. Silver nanoparticles with sizes from 10 to 100 nm are deposited densely on the Si surface, and some of the smaller nanoparticles become embedded in the bulk silicon. After the silver is removed by HNO_3, as shown in Figure 2b, an abundance of nanopores can be observed on the Si surface. From previous reports and our own observations, discussed above, we conclude that the nanopore formation mechanism is Ag-catalyzed in the $HF/AgNO_3$ etchant solution.[16,18] In this case, the $Si/AgNO_3/HF$ system is composed of a corrosion-type redox couple: the cathodic reduction of Ag^+ ions, and its counterpart, the anodic oxidation and dissolution of silicon beneath the deposited Ag.[18,19] At first, the Ag^+ ions of the solution in the vicinity of the Si surface will capture electrons from the Si, and they are then adsorbed on the Si surface as Ag nanoparticles. Simultaneously, the Si underneath the Ag nanoparticles will be oxidized into SiO_2 because the Si will release as many electrons as required by Ag^+ ions. Shallow nanopores immediately form underneath the Ag nanoparticles, due to the etching of SiO_2 by the HF solution. These nanopores become traps of small Ag particles because a particle will not move horizontally after it enters one of the forming pores due to the relatively low-energy barrier for holes in the Ag/Si interface, which is confirmed by the SEM images of the etched Si surface before and after the silver was removed, as shown in Figure 2a and b.[17,18] With longer etching time in the $HF/AgNO_3$ solution, the Ag particles that do not enter the pores grow into branched silver dendrites,[18] and the Ag particles that enter the pores sink into the bulk silicon deeper and deeper.[19]

Figures 3a and b show cross-sectional SEM images of the p-Si (100) surface etched in $HF/AgNO_3$ solution for 4 and 5 min after the deposited Ag is removed. The depth of the etched surface is about 200 nm after 4 min etching and about 250 nm after 5 min. As suggested above, the Ag particles that enter the pores sink into the bulk silicon perpendicularly, so the axis of each nanopore is vertical to the Si surface. The morphology of the Si surface is nearly uniform and the nanopores' diameters are sub-wavelength after etching for either 4 or 5 min. The nanoscale textured silicon surface turns into an effective medium with a gradually varying refractive index, which leads to the low reflectivity (approximately 2%) and black appearance of our samples.[16]

For m-Si, it is difficult to get the pyramid-dotted surface by anisotropic etching because m-Si consists of crystallites with different orientations.[3] So it is more valuable for us to apply this low-cost technique to black-etch m-Si. As shown in **Figure 4**, the hemispheric total reflectance of the m-Si wafer, unetching and after etching for 4 and 5 min is about 28%, 5% and 4%, respectively. This value is not only much lower than

NANO MICRO small

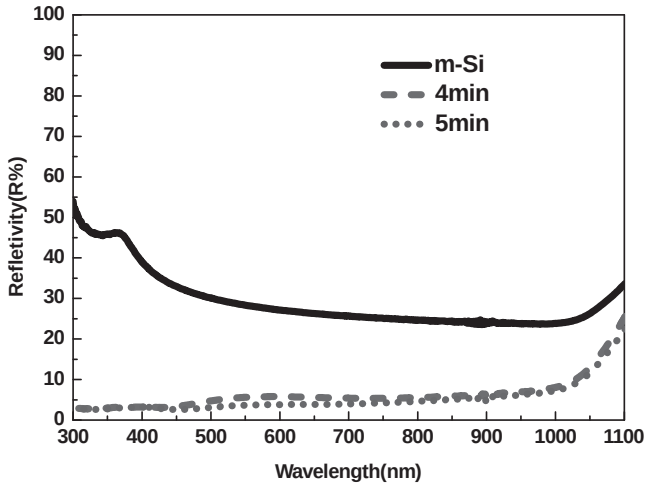

Figure 4. Hemispheric total reflectance of the m-Si wafer, unetched and after etching in $HF/AgNO_3$ solution for 4 and 5 min.

that of the conventional textured samples, whose reflectance is greater than 20%, but also lower than the value of 17.3% obtained by RIE etching for 5 min.[12]

Figures 5a and b show the SEM images of the m-Si after etching in $HF/AgNO_3$ solution for 5 min. Before immersing the m-Si into the $HF/AgNO_3$ solution, the m-Si is etched by $HNO_3/HF/CH_3COOH$ (volume ratio 10:2:5) for 90 s to remove saw damage on the m-Si surface. As shown in Figure 5a, the nanopores form nearly uniformly over the whole area of the m-Si, and the axis of each nanopore is perpendicular to the m-Si surface morphology, but the nanopores near steps are a little broader and deeper than those in the flat area, as shown in Figure 5b. That is because electron exchange between Ag^+ ions and Si is more likely to take place at kinks, steps, and other defects. The Ag nanoparticles tend to form at the kinks, steps, and other defects first, and these initial nanoparticles become bigger than the others and catalyze the oxidation of Si more effectively, as shown in Figure 5c.[19]

For black-silicon-based solar cells, the surface recombination is very serious because of the presence of nanostructures. It is important, therefore, to realize efficient passivation of the nanostructures, as mentioned above. It is well known that thermal oxidation is a very efficient passivation method for silicon-based solar cells. In our study, we find that the nanostructures of black silicon oxidize very much more easily and become covered with more silicon oxide than the bulk silicon. In Figure 5d, we can see that the as-etched sharp nanostructures (in Figure 5b) turn into a smoother morphology after oxidation in oxygen atmosphere at 800 °C for 30 min, which is attributed to the formation of silicon oxide. This is confirmed by the Fourier transform infrared (FTIR) spectra of a series of samples, as shown in **Figure 6**, where the absorption peak at approximately 1068 cm^{-1} is attributed to the asymmetric stretching mode of Si–O–Si.[20] For the as-etched black silicon, a weak peak at approximately 1068 cm^{-1} is observed, suggesting a very thin layer of silicon oxide. This thin layer forms during the chemical etching process, where the $AgNO_3$ is a weak oxidant. The peak at approximately 1068 cm^{-1} of the oxidized bulk silicon at 800°C for 30 min is a little bit stronger than the as-etched sample, indicating that the thermal oxidation is not so effective under this condition. The peak at approximately 1068 cm^{-1} of the black silicon oxidized under the same condition, however, is much bigger than that of the oxidized bulk silicon. This is attributed to the huge specific surface area of the nanostructures, which provides a tremendous number of absorbant sites for molecular oxygen. Therefore, much more oxygen will adsorb on and diffuse into the nanostructures' surfaces than on the bulk silicon, forming a much thicker layer of silicon oxide.

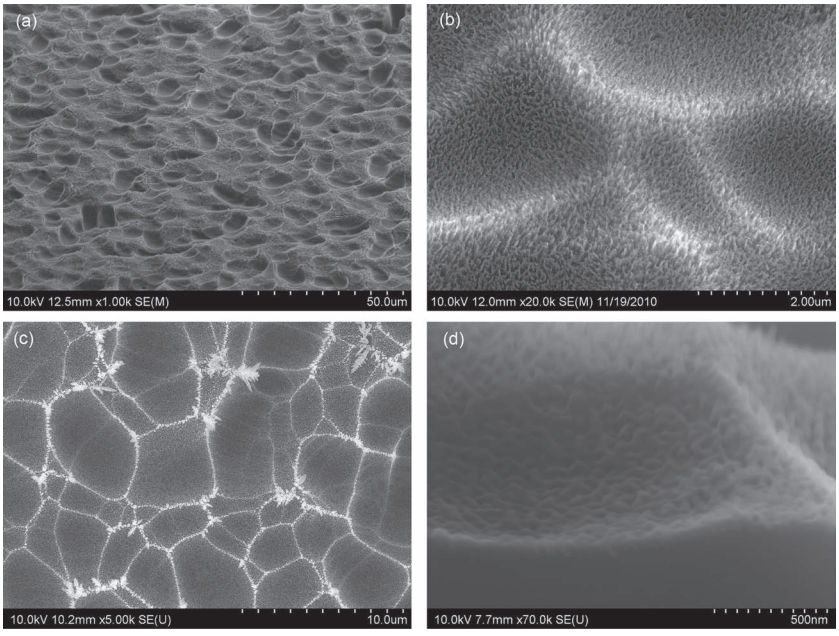

Figure 5. SEM images of m-Si after etching in $HF/AgNO_3$ solution for 5 min: a) large area, b) detail, c) after etching in $HF/AgNO_3$ solution for 30s without removing Ag, and, d) the 5 min black-etched m-Si oxidized at 800 °C for 30 min.

Several solar cells were fabricated and tested based on the black-etched 156 mm × 156 mm m-Si in Tianwei New Energy Holdings Co. At first, the m-Si wafer is etched in $HF/AgNO_3$ solution for 3 min after removing the saw damage. Then standard processes are used to create front phosphorous-diffused emitter, Al back-surface field and screen printed Ag-based front grid on each black-etched wafer. Note that no AR coating or surface passivation is performed during the fabrication of these solar cells. The result measured by using Halm cetisPV-CT-L1 equipment with calibrated 1 Sun simulators shows that conversion efficiency (η) of our solar cell is 11.5%, with open-circuit voltage (V_{oc}) of 575 mV, short-circuit current (J_{sc}) of 26.16 mA cm^{-2} and fill factor (FF) of 76.5%. The low open-circuit

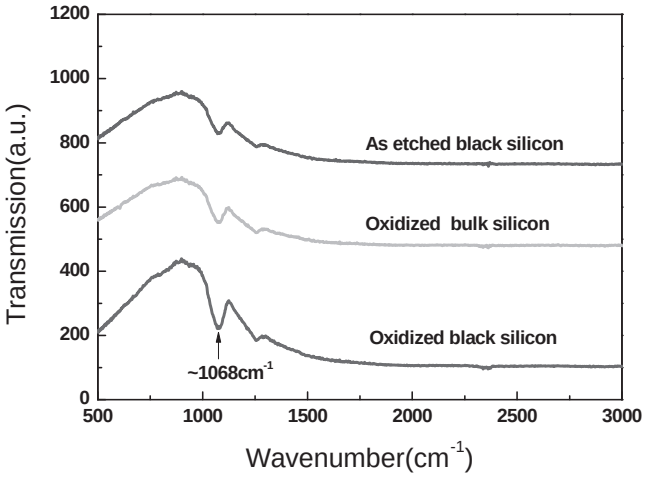

Figure 6. FTIR spectra of the as-etched black silicon and after thermal oxidation.

voltage (V_{oc}) and short-circuit current (J_{sc}) result from the excess carrier recombination at the nanostructured surface of our the solar cell due to the absence of surface passivation. Besides, electrode contact is quite poor between the black surface and the screen printed Ag-based front grid due to the reduced contact area between the nanostructures and the Ag metal.

In order to suppress the surface recombination and obtain good electrode contact, different passivation processes were performed on the black-etched m-Si solar cells. First, 80 nm SiN_x is directly deposited on the phosphorous-diffused m-Si wafer emitter (with square resistivity of 65 Ω/sq), then the standard Al back-surface field and screen printed Ag-based front grid are applied to the m-Si wafer. The conversion efficiency (η) of the cell increased to 14.9% (in comparison with 11.5% for the black silicon cell with no passivation layer), with an open-circuit voltage (V_{oc}) of 596 mV, short-circuit current (J_{sc}) of 32.42 mA cm^{-2} and fill factor (*FF*) of 77.1%. In order to investigate the passivation effects of the SiN_x layer, the cross-sectional SEM image of the sample was obtained as shown in **Figure 7**a. We can see that the SiN_x particles cannot be deposited into the deep and narrow holes or nanopores, indicating that the passivation of nanostructures is not efficient when using SiN_x only.

Our further study reveals that the thermal oxidation followed with deposition of SiN_x is very effective to passivate the nanostructures of black silicon. The thermal oxidation is performed on the 3 min black-etched m-Si wafer under oxygen atmosphere at 800 °C for 20 min. Then 60 nm SiN_x is deposited on this oxidized surface. In Figure 7b, we can see that about an approximately 20 nm thick oxide layer coves the nanostructures, even in the deep and narrow holes. The conversion efficiency (η) of the cell fabricated from this sample is increased to 15.8%, with open-circuit voltage (V_{oc}) of 604 mV, short-circuit current (J_{sc}) of 33.89 mA cm^{-2} and fill factor (*FF*) of 77.3%. The increase of η, V_{oc}, and J_{sc} is attributed to the efficient oxidation passivation of the nanostructure; therefore we conclude that the passivation plays a key role in the fabrication of black silicon solar cells with high conversion efficiency.

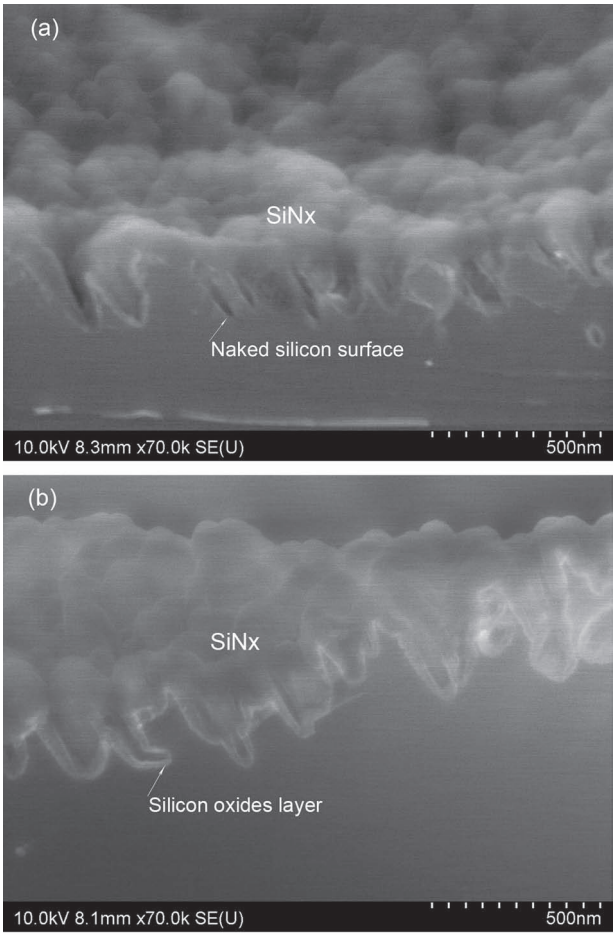

Figure 7. Cross-sectional SEM images of the m-Si coated with: a) 80 nm SiN_x, and, b) 60 nm SiN_x on 20 nm oxide.

More characterization of the black solar cells was carried out to better understand the existing problems for further optimization. **Figure 8** shows the reflection of the black cell with oxide and SiN_x layers in comparison with a conventional m-Si cell. The reflection of the black cell is lower, especially

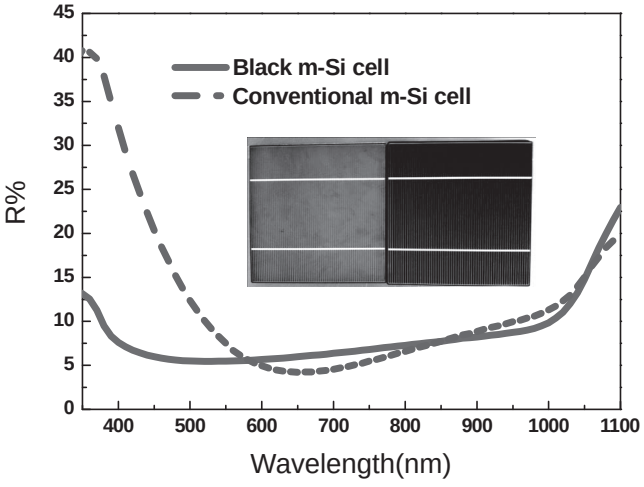

Figure 8. Reflectance of a conventional cell and our m-Si black cell. Inset is a photograph of a conventional cell and our m-Si black cell.

NANO MICRO small

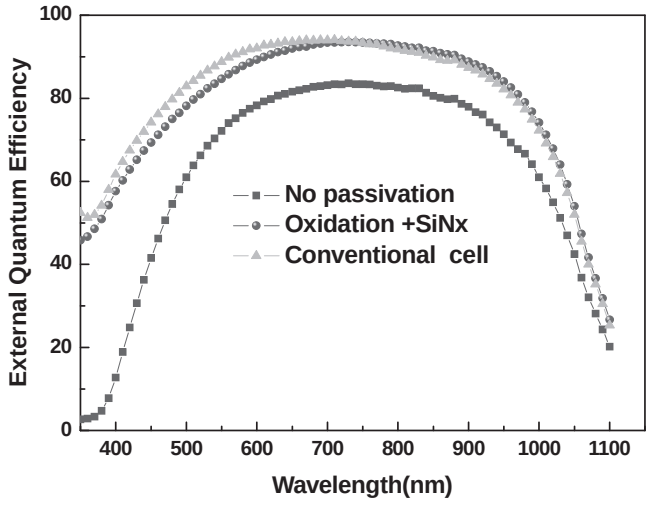

Figure 9. External quantum efficiency (EQE) of 3 min black-etched m-Si solar cells with no passivation, with thermal oxidation and SiN_x passivation, and a conventional cell with SiN_x passivation.

in the short wavelength range. However, the conversion efficiency (η) and other performance of this cell is not as good as the conventional one (16.3%). Here, we attributed this to: i) the deficiency of the current passivation method, and, ii) formation of an excess dead layer during the process of P diffusion in the nanostructure surface, which will affect the short wave response. This is confirmed by the external quantum efficiency (EQE) measurements of cells, as shown in **Figure 9**. The black cell with no passivation layer has a very low EQE. This is because light scattering on the sharp nanostructured layer increases photon path lengths inside the dead layer, worsening EQE loss.[17] This EQE loss is partly reduced after the thermal oxidation because the sharp nanostructures assume a smoother morphology covered with silicon oxide, as shown in Figure 5d.

3. Conclusion

In conclusion, we have demonstrated a promising technique for large-area black silicon fabrication with a low-cost single-step process, both on c-Si and m-Si. When the Si surface is etched by $HF/AgNO_3$ solution for 4 or 5 min, nanopores form in the Si surface with diameters of 50 to 100 nm and depths of 200 to 300 nm. The nanoscale-textured silicon surface turns into an effective medium with a gradually varying refractive index, which leads to the low reflectivity and black appearance of our samples. Surface reflectance was reduced to as low as 2% for c-Si and 4% for m-Si from 300 to 1000 nm, with no antireflective coating. Thermal oxidation passivation is applied to the black silicon nanostructures. Several solar cells were also fabricated based on the 3 min black-etched 156 mm × 156 mm m-Si, and after thermal oxidation and SiN_x passivation, their conversion efficiency (η) increased to 15.8%. For further improvement of the performance of black cells, we suggest that the depth of the nanopores be chosen carefully based on a balance between low reflection and excessive surface recombination due to the formation of the nanostructured layer.[21]

Acknowledgements

This work was supported by the National Science Foundation (grant nos. 61076007, 50532090, 60606023, 10804126, and 10974246), the Ministry of Science and Technology of China (grant nos. 2007CB936203, 2009CB929400, 2009AA033101, and 2011CB302002), and the Chinese Academy of Sciences, as well as the Research Council of Norway through the "NextG" project.

[1] H. Sai, H. Fujii, K. Arafune, Y. Ohshita, Y. Kanamori, H. Yugami, M. Yamaguchi, *Jpn. J. Appl. Phys., Part 1* **2007**, *46*, 3333.
[2] K. Nishioka, T. Sueto, N. Saito, *Appl. Surf. Sci.* **2009**, *255*, 9504.
[3] K. Tsujino, M. Matsumura, Y. Nishimoto, *Sol. Energy Mater. Sol. Cells* **2006**, *90*, 100.
[4] J. Xiao, L. Wang, X. Q. Li, X. D. Pi, D. R. Yang, *Appl. Surf. Sci.* **2010**, *257*, 472.
[5] V. V. Iyengar, B. K. Nayak, M. C. Gupta, *Sol. Energy Mater. Sol. Cells* **2010**, *94*, 2251.
[6] C. H. Lin, D. Z. Dimitrov, C. H. Du, C. W. Lan, *Phys. Status Solidi C* **2010**, *7*, 2778.
[7] R. B. Stephens, G. D. Cody, *Thin Solid Films* **1977**, *45*, 19.
[8] R. Chaoui, B. Mahmoudi, Y. S. Ahmed, *Phys. Status Solidi A* **2008**, *205*, 1724.
[9] J. Yoo, G. Yu, J. Yi, *Mater. Sci. Eng. B* **2009**, *159–160*, 333.
[10] M. Otto, M. Kroll, T. Käsebier, S. M. Lee, M. Putkonen, R. Salzer, P. T. Miclea, R. B. Wehrspohn, *Adv. Mater.* **2010**, *22*, 5035.
[11] J. S. Yoo, I. O. Parm, U. Gangopadhyay, K. Kim, S. K. Dhungel, D. Mangalaraj, Junsin Yi, *Sol. Energy Mater. Sol. Cells* **2006**, *90*, 3085.
[12] J. Yoo, G. Yu, J. Yi, *Sol. Energy Mater. Sol. Cells* **2011**, *95*, 2.
[13] K. S. Lee, M. H. Ha, J. H. Kim, J. W. Jeong, *Sol. Energy Mater. Sol. Cells* **2011**, *95*, 66.
[14] S. Koynov, M. S. Brandt, M. Stutzmann, *Appl. Phys. Lett.* **2006**, *88*, 203107.
[15] S. Koynov, M. S. Brandt, M. Stutzmann, *Phys. Status Solid RRL* **2007**, *1*, R53.
[16] H. M. Branz, V. E. Yost, S. Ward, K. M. Jones, B. To, P. Stradins, *Appl. Phys. Lett.* **2009**, *94*, 231121.
[17] H. C. Yuan, V. E. Yost, M. R. Page, P. Stadins, D. L. Meier, H. M. Branz, *Appl. Phys. Lett.* **2009**, *95*, 123501.
[18] K. Q. Peng, H. Fang, J. J. Hu, Y. Wu, J. Zhu, Y. J. Yan, S. T. Lee, *Chem. Eur. J.* **2006**, *12*, 7942.
[19] K. Q. Peng, J. J. Hu, Y. J. Yan, Y. Wu, H. Fang, Y. Xu, S. T. Lee, J. Zhu, *Adv. Funct. Mater.* **2006**, *16*, 387.
[20] H. J. Chen, X. Y. Hou, G. B. Li, F. L. Zhang, M. R. Yu, X. Wang, *J. Appl. Phys.* **1996**, *79*, 3282.
[21] F. Toor, H. M. Branz, M. R. Page, K. M. Jones, H. C. Yuan, *Appl. Phys. Lett.* **2011**, *99*, 103501.

Received: September 1, 2011
Revised: December 19, 2011
Published online: February 20, 2012

